Available online at www.sciencedirect.com

SciVerse ScienceDirect

Ceramics International 39 (2013) 1567–1574

CERAMICS INTERNATIONAL

www.elsevier.com/locate/ceramint

Mechanical and physical behaviors of short pitch-based carbon fiber-reinforced HfB_2–SiC matrix composites

Shuqi Guo[a,*], Kimiyoshi Naito[a], Yutaka Kagawa[a,b]

[a]*Hybrid Materials Unit, National Institute for Materials Science, 1-2-1 Sengen, Tsukuba, Ibaraki 305-0047, Japan*
[b]*Research Center for Advanced Science and Technology, The University of Tokyo 4-6-1 Komaba, Meguro-ku, Tokyo 153-8505, Japan*

Received 11 June 2012; received in revised form 27 July 2012; accepted 31 July 2012
Available online 11 August 2012

Abstract

Short Pitch-based carbon fiber-reinforced HfB_2 matrix composites containing 20 vol% SiC, with fiber volume fractions in the range of 20–50%, were manufactured by hot-press process. Highly dense composite compacts were obtained at 2100 °C and 20 MPa for 60 min. The flexural strength of the composites was measured at room temperature and 1600 °C. The fracture toughness, thermal and electrical conductivities of the composites were evaluated at room temperature. The effects of fiber volume fractions on these properties were assessed. The flexural strength of the composites depended on the fiber volume fraction. In addition, the flexural strength was significantly greater at 1600 °C than at room temperature. The fracture toughness was improved due to the incorporation of fibers. The thermal and electrical conductivities decreased with the increase of fiber volume fraction, however.

Keywords: B. Composites; C. Electrical conductivity; C. Mechanical properties; C. Thermal conductivity

1. Introduction

Hafnium and zirconium diborides belong to the refractory transition metal deborides from the fourth to the sixth group of the periodic table. Most of these diborides have melting point above 3000 °C, making them potential candidates for thermal protection structures for leading-edge parts on hypersonic re-entry space vehicles at over 1800 °C [1–3]. In particular, hafnium diboride (HfB_2) has higher resistance to oxidation and thermal shock, higher resistance to ablation, compared to zirconium diboride (ZrB_2). However, the use of HfB_2 ceramic materials, even fully densified, in thermomechanical structural applications is limited by their poor fracture resistance and high density as well as degradation of strength at high-temperature.

One of the most promising solutions for improving fracture resistance and lowered density is to apply continuous ceramic fiber to monolithic ceramic for fabricating a fiber-reinforced ceramic matrix composite [4]. Recently, studies with short PAN-based carbon and/or SiC fibers-reinforced ZrB_2 matrix composites showed the improved fracture toughness and lowered density [5–8], as a result of crack bowing, and crack deflection or bridging and low density of fiber. Unfortunately, neither PAN-based carbon fiber nor SiC fiber is suitable for the thermomechanical structural applications above 1600 °C due to significant degradation of the fibers. For comparison, Pitch-based carbon fiber could remain a high strength up to 2000 °C or above without its microstructural degradation. Thus, the Pitch-based carbon fiber should be a suitable reinforcement for the HfB_2-matrix composites. However, the manufacture process, mechanical and physical behaviors of the Pitch-based carbon fiber-reinforced HfB_2 matrix composites are little known.

In the present study, the short Pitch-based carbon fiber-reinforced HfB_2–20 vol% SiC matrix composites, with different fiber volume fractions between 20% and 50%, were manufactured by the hot-press process. The flexural strength of the resulting composites was measured at room temperature and 1600 °C. The fracture toughness, thermal and electrical conductivities of the composites were examined at room temperature. Also, the effects of fiber volume fraction on these properties were discussed.

*Corresponding author. Tel.: +81 29 859 2223; fax: +81 29 859 2401.
E-mail address: GUO.Shuqi@nims.go.jp (S. Guo).

0272-8842/$ - see front matter © 2012 Elsevier Ltd and Techna Group S.r.l. All rights reserved.
http://dx.doi.org/10.1016/j.ceramint.2012.07.108

2. Experimental procedure

The starting powders used in this study were HfB_2 (Grade O, Japan New Metals, Osaka), average particle size ≈ 4.07 μm, α-SiC (UF − 15, H.C. Starck, Berlin, Germany), average particle size ≈ 0.5 μm, and Pitch-based carbon fiber (XNG–90, Nippon Graphite Fiber Corporation, Tokyo), average fiber length ≈ 0.5 mm. The HfB_2 and SiC powders (20% in volume) containing 2 wt% B_4C and 1 wt% C additives were mixed in ethanol using a silicon carbide media for 24 h. Subsequently, the short carbon fibers were added to the as-received HfB_2–20 vol% SiC mixture slurry and the slurry were further mixed to a homogeneous mass using a planetary centrifugal mixer in ambient air for 3 min (ARE–310, Thinky Corporation, Tokyo). The resulting fiber-containing HfB_2–20 vol% SiC slurry was then dried in oven. To examine the effect of fiber volume fraction on the mechanical and the physical behaviors, four compositions of 20, 30, 40 and 50 vol% short Pitch-based carbon fibers-reinforced HfB_2–20 vol% SiC matrix composites (G_f/HfB_2–SiC) were prepared in this study. Hereafter, the four composition G_f/HfB_2–SiC composites are denoted as HSGF20, HSGF30, HSGF40, and HSGF50 (Table 1), respectively.

The obtained powder mixtures were hot-pressed (NEW-HP5, Nissin Giken Co. Ltd., Saitama, Japan) in the graphite dies in tablets averaging 21 mm × 25 mm × 3.5 mm in size. The temperature of the sample was monitored by a two-color optical pyrometer through a hole opened in the die. To obtain highly dense samples, powder compacts were heated to 2100 °C under a pressure of 20 MPa in a flowing Ar atmosphere with a heating rate of ~20 °C/min. After the hot press was held for 60 min, the load was removed and the sample was cooled at ~15 °C/min to 500 °C, and the electric powder was then shut off. The changes in temperature and sintering displacement along the pressure direction were recorded on a computer during the entire sintering process to monitor the densification behavior. After removing the surface of the hot-pressed compacts to avoid contamination from the graphite die, the bulk densities, ρ, of the composite were measured by the Archimedes method with distilled water as the medium. The theoretical densities of the composites were calculated according to the rule of mixtures. Density values of 11.2 g/cm^3 for HfB_2, 3.22 g/cm^3 for SiC, 2.52 g/cm^3 for B_4C, 1.8 g/cm^3 for C, and 2.12 g/cm^3 for Pitch-based carbon fiber are used in the calculation of theoretical density of the composites. The microstructure of the resulting composites was characterized by field emission scanning electron microscopy (FE-SEM). The grain sizes, d, of HfB_2 and SiC in the matrix were determined by measuring the average linear intercept length, d_m, of the grains in FE-SEM images of the composites, according to the relationship of $d = 1.56 d_m$ [9].

The flexural strengths of the composites were measured on specimens averaging 25 mm × 2.5 mm × 2 mm in size using four-point flexure (inner span 10 mm, outer span 20 mm) at

Table 1
The compositions, densities, average grain diameter, fracture toughness, thermal and electrical conductivities of short Pitch-based carbon fiber-reinforced HfB_2-20 vol% SiC matrix composites consolidated by hot-pressing.

Materials	Fiber content f (vol%)	Bulk density (g/cm^3)	Real density (g/cm^3)	Relative density (%)	Average grain diameter, d (μm)		Fracture toughness K_C (MPa m$^{1/2}$)	Thermal conductivity k_m (W (m K)$^{-1}$)	Electrical conductivity σ (Ω^{-1} cm^{-1})
					HfB_2	SiC			
HSGF20	20	7.24	7.28	99.5	2.63 ± 1.17	1.29 ± 0.51	5.6 ± 0.2	93.8	1.76×10^4
HSGF30	30	6.59	6.64	99.3	2.63 ± 1.01	1.46 ± 0.57	5.7 ± 0.3	73.9	1.45×10^4
HSGF40	40	5.89	5.99	98.3	2.64 ± 0.98	1.54 ± 0.76	5.9 ± 0.3	67.1	1.01×10^4
HSGF50	50	5.24	5.34	98.1	2.66 ± 1.29	1.58 ± 0.66	6.1 ± 0.2	54.4	0.67×10^4

room temperature and 1600 °C, in flowing Ar atmosphere. The bend test was performed using an Instron testing system (Model-4505, Instron Co., Ltd., Canton, MA, USA) with a crosshead speed of 0.5 mm/min. At least five specimens were used for each measurement. After the bending test, the fracture surface of specimens was examined using scanning electron microscopy (SEM). In addition, the fracture toughness of the composites was determined on the same four-point bending test at room temperature using a single edge notched beam (SENB) specimen with a notch of ~0.8 mm in depth and 0.15 mm in thickness [10].

The thermal conductivity of the composites, k_m, is determined from the thermal diffusivity, α, heat capacity, C_p, and density, ρ, according to the following equation [11]:

$$k_m = \rho C_p \alpha \quad (1)$$

The thermal diffusivity was measured on a disk-shaped specimen with a diameter of 10 mm and a thickness of ~2 mm using the nanoflash technique (LFA447/2-4N, Nanoflash, NETZSCH-Geratebau GmbH, Postfach, Germany). Prior to the measurements, the samples were coated with a colloidal graphite spray to enhance the absorption of the Xenon light pulse energy and the emission of IR radiation to the temperature detector. The heat capacity was determined with alumina as the reference material.

Moreover, the electrical conductivity measurements of the composites were performed using the standard four-point probe method at room temperature to reduce the effects of contact resistance. A power supply (Model: 6220, Keithley, Cleveland, Ohio, USA) and digital multimeter (Model: 2182 Nanovoltmeter, Keithley) were used to measure the *I–V* characteristics of the samples. The detailed measurement procedures for the thermal and electrical conductivities had been reported elsewhere [12].

3. Results and discussion

3.1. Densification and microstructure

The typical shrinkage curves obtained during the hot pressing cycle for the four composition composites are shown in Fig. 1. It is found that the shrinkage behavior of the composites was linked to fiber volume fraction. The measurable shrinkage was initially observed at a temperature range between 1490 °C and 1820 °C for the four composition composites, depending on fiber volume fraction. The onset temperature of densification was determined to be ~1490 °C for HSGF20, ~1510 °C for HSGF30, ~1550 °C for HSGF40, and ~1820 °C for HSGF50. It is evident that the onset temperature of densification was raised with increase of fiber volume fraction. In particular, for HSGF50 the onset temperature of densification was significantly raised and it was ~270 °C higher than that of HSGF40. This indicated that the densifying mechanism of the HfB_2–SiC matrix powder, such as grain boundary diffusion and grain boundary migration, was inhibited due to the presence of fiber. The activated temperature of the

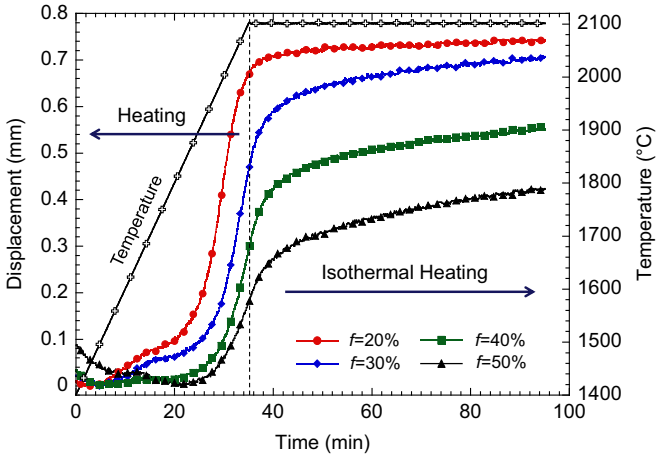

Fig. 1. Typical shrinking curves obtained during the hot-pressing cycle for the short Pitch-based carbon fiber-reinforced HfB_2–20 vol% SiC matrix composites.

densification mechanism shifted to a higher temperature with increase of fiber volume fraction. During the subsequent densification, although the densification mechanism of the matrix was activated, only a slow shrinkage was observed for the composites until ~1900 °C. Then, a rapid shrinkage occurred with a further increase of temperature. In the rapid shrinkage stage, the shrinkage rate depended on the fiber volume fraction and it decreased with the increase of fiber volume fraction. This indicated that the presence of fiber hindered the densification progress of the matrix. In addition, the observed rapid shrinkage region was very narrow. For HSGF20, the rapid shrinkage almost ended when the temperature approached to 2100 °C. For the other composition composites, the rapid shrinkage ended after the holding time of ~5 min at 2100 °C.

Moreover, the densification of the four composition composites was not completed during the heating and the densification carried out continuously during the subsequent isothermal heating. For HSGF20, the main part of densification occurred during heating. The noticeable shrinkage was observed only within ~10 min followed by the isothermal heating, and then a plateau was observed in the curve. For the other composites, however, the shrinkage proceeded during the isothermal heating until the end of sintering, without the plateau in the curve. The measured densities of the four composition composites consolidated by the hot-press process are summarized in Table 1. Relative density exceeding 98% was obtained for the four composition composites at 2100 °C for 60 min. This indicated that highly dense composite compacts could be manufactured, by using the hot press process.

Fig. 2 showed typical examples of FE-SEM images of the microstructures for the four composition composites. It is found that the short fibers were randomly and uniformly dispersed in the matrix without the clumps of fibers (Fig. 2(a) and (b)) in all the resulting composites. The absence of the fiber clumps suggests that the short fibers were homogeneously dispersed in the matrix slurry after the mixing. This indicated

that the mixing method used in this study is very effective for homogeneously dispersing short fibers in ceramic slurry although the mixing time was very short (only 3 min). This short mixing time may reduce the damage of fibers due to mixing, therefore improved mechanical properties. In addition, the defects such as pores and cracks were not observed, showing highly dense composites, which agrees with the measured high densities (Table 1). Under high-magnification (Fig. 2(c)), it is found that the matrix showed a homogeneous and fine grain microstructure and it consisted of the equiaxed HfB_2 (brighter contrast) and SiC (dark contrast) grains. The measured grain sizes of HfB_2 and SiC in the composites were summarized in Table 1. It is found that the average grain diameter of HfB_2 in the composites was almost the same (Table 1), regardless of fiber volume fraction. The average grain diameter of HfB_2 is ~2.6 μm, which is substantially smaller than that of the starting powder (~4.1 μm). Apparently, the mixing process is effective in reducing the size of HfB_2 particles. For comparison, the SiC grain in the composites coarsened with increasing fiber volume fraction, with particles size range of 1.3–1.6 μm which is larger than that of the starting powder (~0.5 μm). This suggests that the addition of fiber hindered from breaking apart the agglomeration of SiC particles during the mixing process. As a result, clusters of SiC particles were fused together during hot pressing to form larger SiC particles. Furthermore, the hindered effect is enhanced with increasing fiber volume fraction.

Fig. 3 shows typical examples of FE-SEM micrographs near the boundary between the fiber and the matrix for a longitudinal fiber and transverse fiber in the composites. In the cross-section (Fig. 3(a)), the surface of fiber exhibits an inherent saw-toothed front shape. A noticeable interface reaction layer was not showed between the fiber and the matrix, however. This indicated that Pitch-based carbon fiber is chemically stable and no significant reaction occurred during the hot-press at 2100 °C. For comparison, an earlier study in a PAN-based carbon fiber-reinforced ZrB_2–SiC composite consolidated by hot-press at 2000 °C showed the presence of the interfacial reaction layer between the fiber and matrix [5]. In the plan-section (Fig. 3(b)), the fibers appear to be uniform in structure. This suggests that there is little difference in microstructure across the fiber section. In addition, a lot of thin layers were observed on the longitudinal section of the fiber, showing that microstructure of the fiber consisted of layers. An early study in the microstructures of Pitch-based fibers showed that the fibers have a sheet-like microstructure [13], and the crystallite sheets were well-defined and less curved, as a result of its high modulus (E_f=880 GPa). Additionally, there are gaps between the crystallite sheets, which led to pull out of the sheets at failure.

3.2. Mechanical and physical behaviors

Fig. 4 shows plots of the four-point flexural strengths as a function of fiber volume fraction for the composites tested at room temperature and 1600 °C. It is found that the room temperature flexural strength of the composites

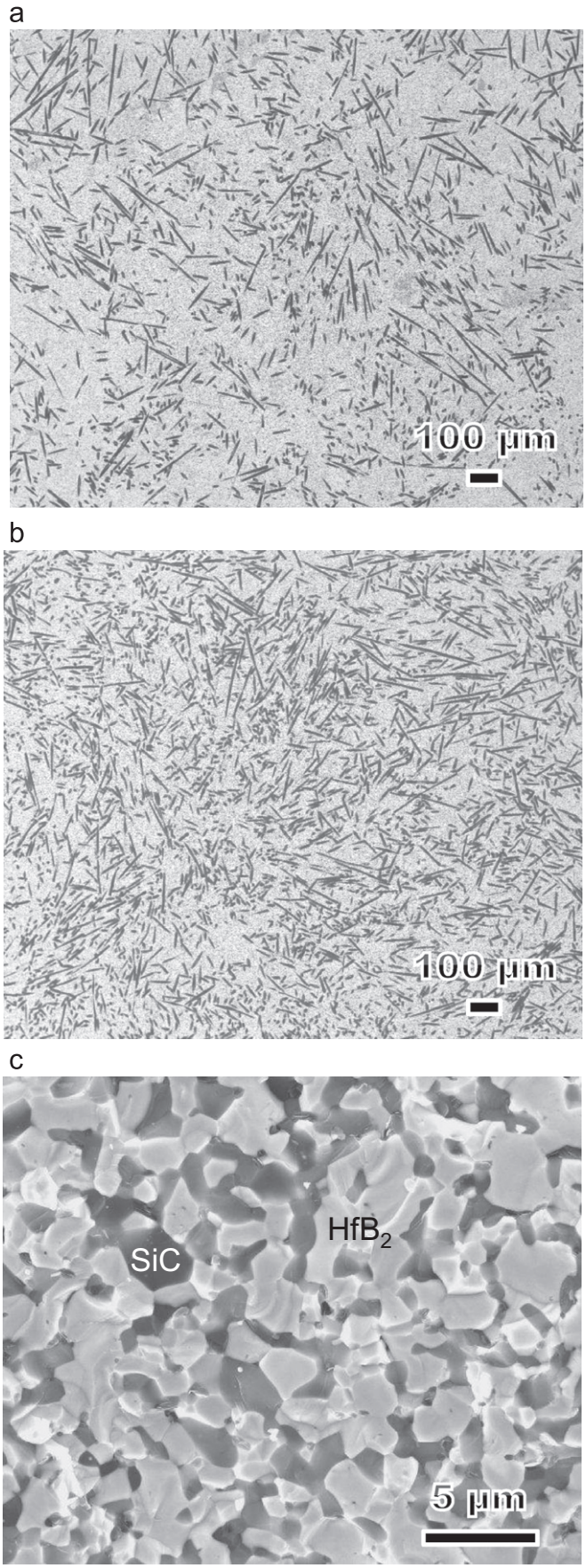

Fig. 2. Typical examples of FE-SEM micrographs of the microstructures for the composites; (a, c) HSGF20, and (b) HSGF40.

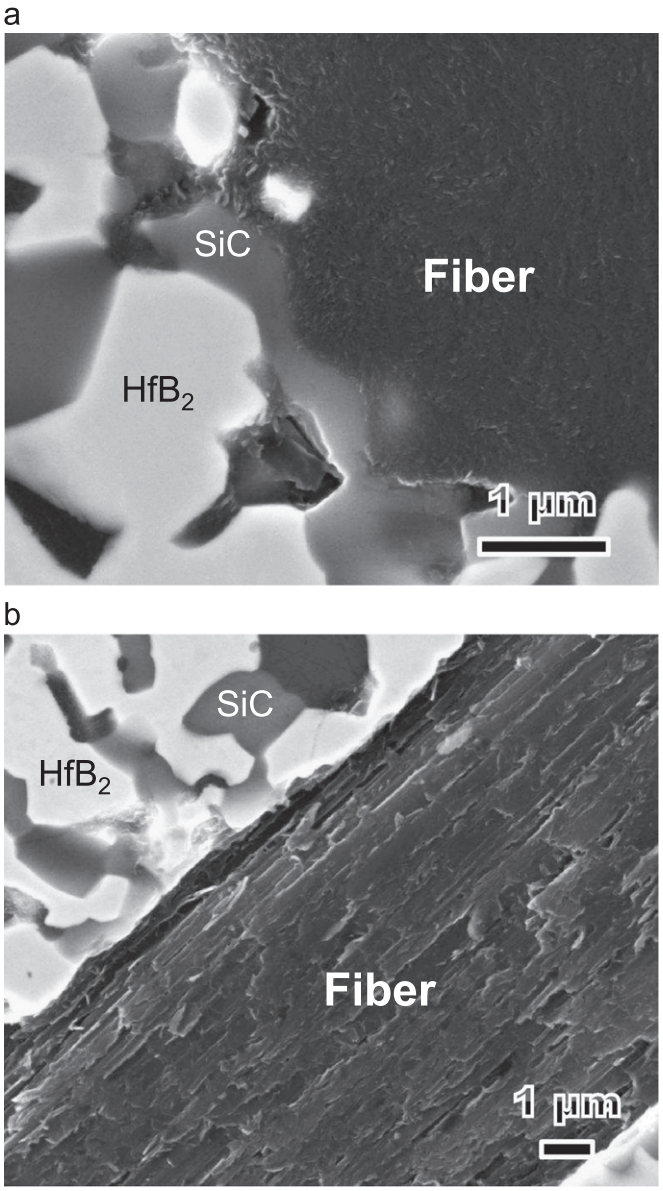

Fig. 3. High-magnification FE-SEM micrographs of the interface between the fiber and the matrix for the composite (HSGF20), (a) cross-section, and (b) plan-section.

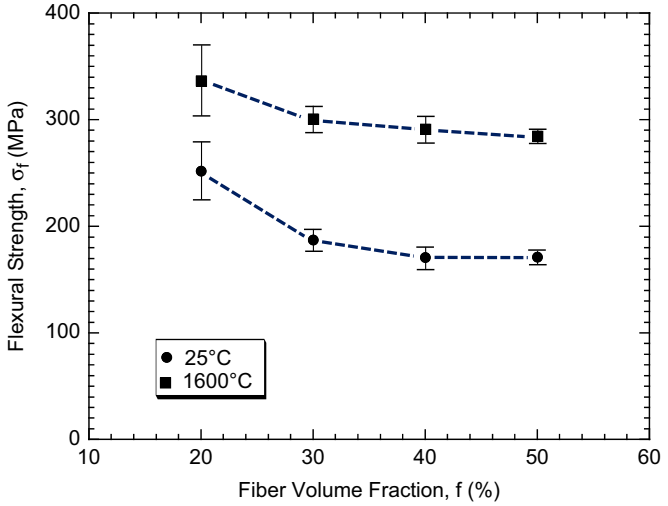

Fig. 4. Plots of the four-point flexural strengths as a function of fiber volume fraction for the composites tested at room temperature and 1600 °C.

was lower than that reported previously for the monolithic HfB_2–20 vol% SiC ceramic. Gasch et al. [14] showed that the four-point flexural strength at room temperature was ~450 MPa for the monolithic HfB_2–20 vol% SiC ceramic consolidated by hot pressing at 2200 °C for 1 h, with grain size range of 10–20 μm for HfB_2 and 2–10 μm for SiC. It is evidence that the average grain sizes of HfB_2 and SiC are larger in the monolithic ceramic than in the composites investigated in the present study (Table 1). Apparently, although the grain sizes of HfB_2 and SiC in the composites investigated in this study were smaller those reported in the monolithic HfB_2–20 vol% SiC ceramic, the flexural strength of the composite was lower that of monolithic ceramic. An early study in the monolithic ZrB_2–30 vol% SiC ceramics showed that the flexural strength increased with reduction of ZrB_2 and/or SiC grain size [15]. Hence, presumably, the reduction in the strength of the composites due to addition of fiber was associated with the presence of the thermal residual stress by thermal expansion misfit between the fiber and the matrix. Increasing fiber volume fraction from 20% to 30% led to a significant reduction of the flexural strength. However, further increase of fiber volume fraction led to a slight reduction of the strength. In particular, for the fiber volume fraction greater than 40 vol%, the flexural strength remains almost constant, independent on the fiber volume fraction. Similar dependency of the flexural strengths on fiber volume fraction was also observed for the samples fractured at 1600 °C. Presumably, the reduction in the strength of the composite with fiber volume fraction is attributed to the increase of SiC grain size (Table 1) because smaller SiC grain size would result in even higher strength for HfB_2–SiC [15]. The flexural strengths of the composites were significantly higher at 1600 °C than at room temperature, however. For comparison, an earlier study in monolithic HfB_2-15 vol% SiC ceramics showed a significant drop in flexural strength above 1000 °C [16], as a result of softening of a grain boundary phase at high temperatures.

It is well-known that the flexural strength of the composites depended on fibers, interface and internal residual stress. In the present study, the Pitch-based carbon fiber used has stable physical and chemical properties during the hot pressing process of 2100 °C. Neither significant strength drop of fiber nor serious interface reaction between the fiber and the matrix could be expected after hot-press. However, a huge internal residual tensile stress could be expected in the composites, resulting from the difference of thermal expansion coefficients between the fiber and the matrix. It is known that the thermal expansion coefficient is approximately equal to zero for the Pitch-based carbon fiber and is $7.0 \times 10^{-6}\,K^{-1}$ at 1600 °C for the matrix [14]. This suggests that the large residual tensile stress were produced in the

matrix upon cooling from the processing temperature to room temperature. The residual tensile stress is roughly calculated by the following equation [17]:

$$\sigma_r = fE_f \Delta T \Delta\alpha \quad (2)$$

where E_f is Young's modulus of fiber (E_f=880 GPa), ΔT and $\Delta\alpha$ are the temperature difference and the thermal expansion difference, respectively. At room temperature, the residual tensile stress in the matrix yielded the range of 2.6–6.4 GPa, and it increased with the increase of fiber volume fraction. The presence of the tensile stress led to the decreased strength. At 1600 °C, however, the residual tensile stress are significantly relaxed, therefore the increased strength.

In addition, the resulting composites showed the improved fracture resistance (Table 1) due to the incorporation of fibers. The fracture toughness was in the range of 5.7–6.1 MPa $m^{1/2}$ for fiber volume fractions between 20% and 50%. Compared with the monolithic HfB_2–20 vol% SiC ceramic (K_C=4 MPa $m^{1/2}$ [14]), the corresponding increase of the fracture toughness was ~40% for HSGF20, ~43% for HSGF30, ~48% for HSGF40, and ~53% for HSGF50. It is evident that this improvement is attributed to the crack deflection and/or bridging [5–8]. The fracture surfaces of the composites fractured at room temperature and 1600 °C were examined under FE-SEM, typical examples are shown in Fig. 5. The fracture surface is jagged and stepped across the thickness, and there were fibers pull-out. This fracture behavior was observed for all the samples fractured at room temperature and at 1600 °C. Increasing fiber volume fraction led to a more jagged and stepped fracture surface (Fig. 5(c) and (d)). Under high-magnification, it is seen that the fiber pull-out did not occur at the interface, but between the sheets which consisted of fiber adjacent to the interface (Fig. 6(a) and (b)). In addition, the pull-out of the sheets was observed on the fracture surface of the fibers (Fig. 6(a)). This suggests that the interfacial bond is stronger than the bond between the sheets of fiber due to the presence of gaps between the sheets (Fig. 3(b)). It is evident that the interface between the fiber and the matrix could effectively transfer load from the matrix to the fiber. Furthermore, for the sample fractured at 1600 °C, the fracture surface has more dimples (Fig. 5(b) and (d)) because the intergranular fracture was dominative for the matrix at 1600 °C (Fig. 6(d)). For comparison, the intragranular fracture was governable for the matrix at room temperature (Fig. 6(c)).

The measured thermal and electrical conductivities of the composites are summarized in Table 1. The composites showed a good thermal conductivity, with thermal conductivities in the range of 54.4–93.8 W/m K, dependent on the fiber volume fraction. The thermal conductivity of the composites is higher than that of the monolithic HfB_2–20 vol% SiC ceramic consolidated with commercially available HfB_2 and SiC powders by hot-press [14] although which is composed of the larger equiaxed HfB_2 (diameter: 10–20 μm) and SiC (diameter: 2–10 μm) grains. In the studied composites, the

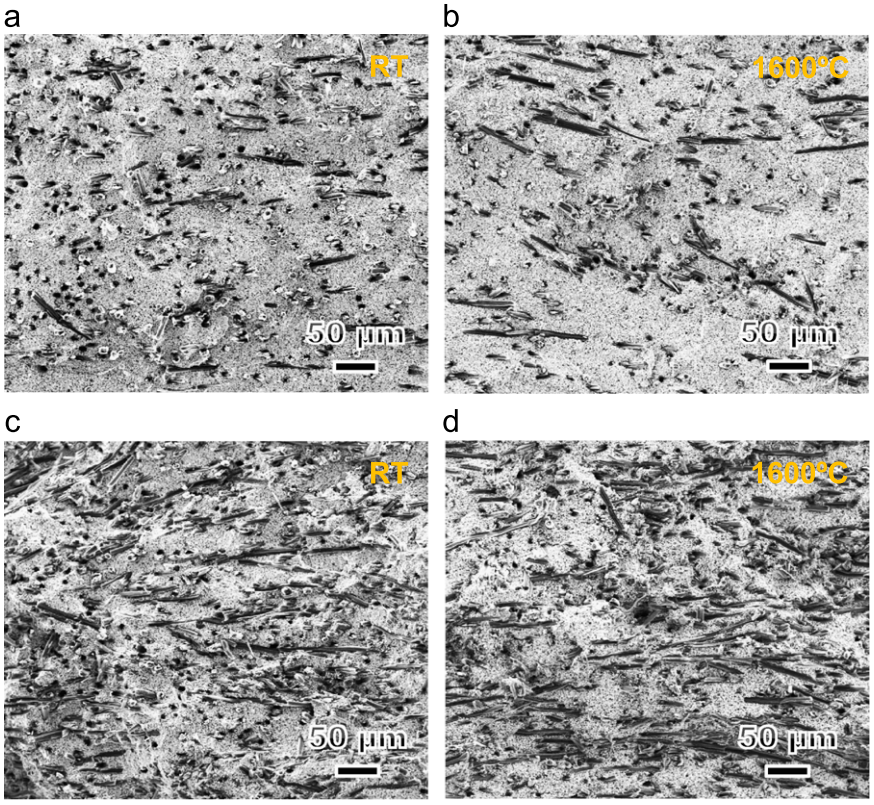

Fig. 5. Typical examples of FE-SEM micrographs of the fracture surfaces for the composites tested at room temperature (a, c) and 1600 °C (b, d); (a, b) HSGF20, and (c, d) HSGF40.

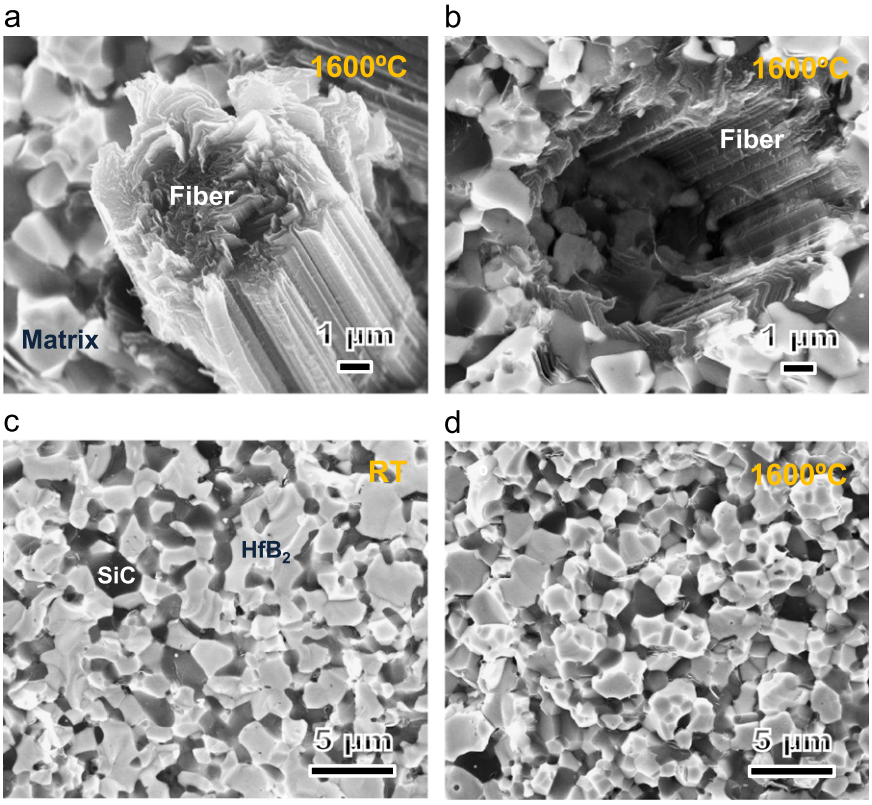

Fig. 6. High-magnification FE-SEM micrographs of the fracture surfaces for the composite (HSGF20) tested at room temperature and 1600 °C, showing the fracture fashions of the fiber and the matrix.

increase in thermal conductivity due to the addition of fiber is believed to be attributed to the high thermal conductivity of fiber (500 W/m K). However, increasing fiber volume fraction led to a significant decrease in the thermal conductivity, as a result of the presence of interfacial thermal resistance at the fiber/matrix interface. An early study in carbon nanotube (CNT)-reinforced SiO_2 matrix composites [18] showed that the decreased thermal conductivity with CNT could be due to a high interface thermal resistance across the interfaces. It is evident that the interfacial thermal resistance increased with fiber volume fraction, therefore decreased thermal conductivity. In addition, the electrical conductivities of the composites decreased with the increase of fiber volume fraction. However, the conductivities observed were in the range of conductor materials, showing a good electrical conductivity.

4. Conclusions

In summaries, highly dense short Pitch-based carbon fiber-reinforced HfB_2–20 vol% SiC matrix composites were prepared by hot-press process at 2100 °C and 20 MPa for 60 min. The composite microstructure exhibited that the short fibers were randomly and uniformly embedded in a homogeneous equiaxed grains matrix microstructure. The significant interface reaction layer was absent between the fiber and the matrix. The flexural strength at room temperature and at 1600 °C decreased as the fiber volume fraction increased from 20% to 40%; however, the strength remained nearly the constant as the fiber volume fraction was greater than 40%. Furthermore, the flexural strength was greater at 1600 °C than at room temperature. This should be attributed to the relaxation of the large residual tensile stress in the matrix at 1600 °C. The fracture toughness was significantly improved due to the addition of fibers. The thermal conductivity decreased with the increase of fiber volume fraction, with the range 54.4–93.8 $W\,(m\,K)^{-1}$. In addition, the electrical conductivity decreased with the increase of fiber volume fraction, with the range 0.67×10^{4}–1.76×10^{4} $(\Omega\,cm)^{-1}$.

References

[1] K. Upadhya, J.-M. Yang, W.P. Hoffmann, Materials for ultrahigh temperature structural applications, American Ceramic Society Bulletin 76 (1997) 51–56.
[2] E. Wuchina, E. Opila, M. Opeka, W. Fahrenholtz, I. Talmy, UHTCs: ultra-high temperature ceramic materials for extreme environment applications, Interface 16 (2007) 30–36.
[3] A. Paul, D.D. Jayaseelan, S. Venugopal, E. Zapata-Solvas, J. Binner, B. Vaidhyanathan, A. Heaton, P. Brown, W.E. Lee, UHTS composites for hypersonic applications, American Ceramic Society Bulletin 91 (2012) 22–29.
[4] W.C. Tu, F.E. Lange, A.G. Evans, Concept for a damage – tolerant ceramic composite with a strong interfaces, Journal of the American Ceramic Society 79 (1996) 417–424.
[5] F. Yang, X. Zhang, J. Han, S. Du, Processing and mechanical properties of short carbon fibers toughened zirconium diboride-based ceramics, Materials and Design 29 (2008) 1817–1820.

[6] F. Yang, X. Zhang, J. Han, S. Du, Characterization of hot-pressed short carbon fiber reinforced ZrB_2–SiC ultra−high temperature ceramic composites, Journal of Alloys and Compounds 472 (2009) 395–399.
[7] H. Hu, Q. Wang, Z. Chen, C. Zhang, Y. Zhang, J. Wang, Preparation and characterization of C/SiC−ZrB_2 composites by precursor infiltration and pyrolysis process, Ceramics International 36 (2010) 1011–1016.
[8] D. Sciti, S. Guicciardi, L. Silvestroni, SiC chopped fibers reinforced ZrB_2: effect of the sintering aid, Scripta Materialia 64 (2011) 769–772.
[9] M.I. Mendelson, Average grain size in polycrystalline ceramics, Journal of the American Ceramic Society 52 (1969) 443–446.
[10] L.A. Simpson, Use of the notched-beam test for evaluation of fracture energies of ceramics, Journal of the American Ceramic Society 57 (1974) 151–154.
[11] W.J. Parker, W.J. Jenkins, C.P. Butler, G.L. Abbott, Flash method of determining thermal diffusivity, heat capacity and thermal conductivity, Journal of Applied Physics 32 (1961) 1679–1684.
[12] S.Q. Guo, T. Nishimura, Y. Kagawa, H. Tanaka, Thermal and electric properties in hot-pressed ZrB_2−$MoSi_2$−SiC composites, Journal of the American Ceramic Society 90 (2007) 2255–2258.
[13] K. Naito, Y. Tanaka, J.-M. Yang, Y. Kagawa, Tensile properties of ultrahigh strength PAN-based, ultrahigh modulus Pitch-based and high ductility Pitch-based carbon fibers, Carbon 46 (2008) 189–195.
[14] M. Gasch, D. Ellerby, E. Irby, S. Beckman, M. Gusman, S. Johnson, Processing, properties and arc jet oxidation of hafnium diboride/silicon carbide ultra high temperature ceramics, Journal of Materials Science 39 (2004) 5925–5937.
[15] A. Rezaie, W.G. Fahrenholtz, G.E. Hilmas, Effect of hot pressing time and temperature on the microstructure and mechanical properties of ZrB_2−SiC, Journal of Materials Science 42 (2007) 2735–2744.
[16] R. Loehman, E. Corral, H.P. Dumm, P. Kotula, R. Tandon, Ultra High Temperature Ceramics for Hypersonic Vehicle Applications, SANDIA REPORT, No. SAND 2006−2925, Sandia National Laboratories, California, USA, 2006.
[17] W.A. Curtin, B.K. Ahn, N. Takeda, Modeling brittle and tough stress-strain behavior in unidirectional ceramic matrix composites, Acta Materialia 46 (1998) 3409–3420.
[18] R. Sivakumar, S.Q. Guo, T. Nishimura, Y. Kagawa, Thermal conductivity in multi-wall carbon nanotube-silica-based nanocomposites, Scripta Materialia 56 (2007) 265–268.